Ceramics International xxx (xxxx) xxx–xxx

Contents lists available at ScienceDirect

Ceramics International

journal homepage: www.elsevier.com/locate/ceramint

Thermally stable boron-containing mullite fibers derived from a monophasic mullite sol

Xiaolei Song, Yangrui Gao, Qiang Liu, Juan Wang, Shuwei Yao, Wensheng Liu*, Yunzhu Ma*, Qingshan Cai*

State Key Laboratory of Powder Metallurgy, Central South University, Changsha 410083, China

ARTICLE INFO

Keywords:
Mullite
Fibers
Monophasic sol
Thermal stability
Microstructure
Tensile strength

ABSTRACT

In this work, we reported the synthesis of monophasic boron-containing mullite (MBM) fibers using basic aluminum acetate (BAA) and tetraethyl orthosilicate (TEOS) as starting materials and performed a comparative study between our newly synthesized MBM and commercial Nextel™ 312 fibers. The morphology and the tensile strength are investigated for the new MBM fibers. Continuous and uniform green fibers with a smooth surface were produced via hand drawing method. After the pyrolysis process, amorphous inorganic MBM fibers with a tensile strength of 1.18 ± 0.17 GPa were obtained. After various heat treatment processes (1000–1400 °C for 1.5 h), we found the mullite formation temperature is within the temperature range from 1050 to 1075 °C for both MBM and Nextel™ 312 fibers. However, the results show that the MBM fibers fabricated in this study have a better thermal stability than Nextel™ 312 fibers despite the fact both have the same chemical composition. The improved stability of our MBM fibers is owing to their higher $Al_4B_2O_9$ formation temperature and lower $Al_{18}B_4O_{33}$ decomposition rate in comparison to those of Nextel™ 312 fibers. Moreover, the newly synthesized MBM fibers have more stable microstructure and less loss in tensile strength at elevated temperatures.

1. Introduction

Continuous mullite ($3Al_2O_3{\cdot}2SiO_2$) fibers are an important type of ceramic materials for their extensive application in areas such as insulation, filtration, catalyst, or wide use as reinforcements for ceramic matrix composites (CMCs), etc. [1–4]. They have drawn great research attention in recent years due to their excellent dielectric properties, low thermal conductivity, low thermal expansion coefficient, outstanding chemical stability, as well as good thermal stability under high-temperature circumstance [5,6]. Many commercial mullite fibers with different chemical compositions and specific performance have been successfully developed. Among those products, Nextel™ 312 fibers (short for 312 fibers) manufactured by 3 M Company have competitive advantages for their extreme lightweight and superior flexible features. Those advantages can be ascribed to the introduction of 14 wt% B_2O_3 [7–9]. Their density, as reported, is of 2.7 g/cm^3, which is much lower than other brands of mullite fibers. The low density is likely to reduce the total weight of composite materials composed of a large amount of such fibers. In addition, 312 fibers are mainly at the amorphous state and have a Young's modulus of ~ 150 GPa [1,3], which display the best flexibility among all the commercial mullite fibers. Good flexibility enables the fibers to be converted into desired shapes or forms.

Despite those advantages, a huge challenge of 312 fibers still exists, that is their relatively poor thermal stability under high-temperature conditions [1,8]. The poor thermal stability of 312 fibers is caused by the early formation of unstable alumina borate before the mullite formation [10,11]. As a typical example, $Al_4B_2O_9$ forms at ~ 885 °C [12], a little lower than the formation temperature of γ-Al_2O_3 (~ 920 °C) and much lower than the mullite formation temperature (~ 1250 °C) of pure commercial mullite fibers [13]. $Al_4B_2O_9$ will decompose into $Al_{18}B_4O_{33}$ and B_2O_3, and $Al_{18}B_4O_{33}$ further decompose into Al_2O_3 and B_2O_3. Those alumina borate phases also greatly reduce the mullite formation temperature by providing an epitaxial substrate for mullite nucleation and growth [14,15]. The early formation of crystallized mullite phase consumes the amorphous phase, resulting in coarser grains and more defects like voids and cracks. As a result, the mechanical properties of the fibers degrade, especially at a higher temperature.

Another shortcoming of 312 fibers is a complex, delicate and high-cost manufacturing process [12,16]. It is known that mullite can be synthesized through diphasic and monophasic sol-gel route [13]. Most commercial mullite fibers are produced through the diphasic mullite

* Corresponding authors.
E-mail addresses: liuwensheng@csu.edu.cn (W. Liu), zhuzipm@csu.edu.cn (Y. Ma), caiqingshan@csu.edu.cn (Q. Cai).

https://doi.org/10.1016/j.ceramint.2018.09.301
Received 2 August 2018; Received in revised form 25 September 2018; Accepted 29 September 2018

sol-gel route and 312 fibers are one of this kind. For instance, alumina sol and colloidal silica are separately prepared to acquire spinnable sol. Before mixing, the surface potential of the colloidal particles for the two sols must be adjusted to be the same, otherwise, sediments will appear. Moreover, the as-spun gel fibers are hydrophilic due to the existence of silica gel, and thus cannot be exposed to the environment with high humidity before pyrolysis. On the contrary, the monophasic route is a simple, stable and low-cost process. The sources of alumina and silica are hydrolyzed simultaneously without any post-treatment during the preparation of monophasic mullite sol. The most commonly used silica source is tetraethyl orthosilicate (TEOS), which is much cheaper than colloidal silica. In addition, the gel fibers are less sensitive to environmental humidity.

For pure mullite fibers, the diphasic sol-gel route leads to higher mullite formation temperatures than the monophasic sol-gel route. When adopts the diphasic sol-gel route, however, the B_2O_3 addition decreases the mullite formation temperature seriously (~ 150 °C with 5 wt% B_2O_3) [15]. On the other hand, the monophasic sol-gel route is less sensitive to the B_2O_3 addition in the mullite formation temperature [17]. In our previous work, electrospun mullite-type (Al_2O_3-SiO_2-B_2O_3) nanofibers with Al_2O_3:SiO_2:B_2O_3 mol ratio of 3:2:1 had been successfully fabricated through monophasic route [18]. We found that mullite phase was detected at 1100 °C and amorphous SiO_2 remained in the sample prepared at 1400 °C. Nevertheless, the thermal stability of mullite fibers with B_2O_3 addition has yet to be understood for both diphasic and monophasic sol-gel routes, and its influence on the mechanical performance of mullite fibers at high temperature is still unclear.

In present work, boron-containing mullite fibers with the same chemical composition with 312 fibers were synthesized through a monophasic mullite route via hand drawing method. Basic aluminum acetate (BAA) $(Al(OH)_2(OOCCH_3)\cdot 1/3H_3BO_3$, boric acid acted as the stabilizer) and tetraethyl orthosilicate (TEOS) were used as the raw materials. The microstructure and tensile strength of the monophasic boron-containing mullite (MBM) fibers after heat-treatment at elevated temperatures were investigated. For comparison, commercial 312 fibers were conducted with the same heat-treatment. The thermal stability of our MBM fibers and 312 fibers is discussed in detail and its influence on the mechanical performance at high temperature is uncovered.

2. Experimental

2.1. Materials

Basic aluminum acetate (BAA) $(Al(OH)_2(OOCCH_3)\cdot 1/3H_3BO_3$, boric acid acted as the stabilizer) used as the source of alumina and borate oxide was supplied by Strem Chemicals, Inc. (Boston, USA). Tetraethyl orthosilicate (TEOS, SiO_2 content = 28 wt%) used as the source of silica was offered by Xilong Chemical Co., Ltd. (Guangzhou, China). Absolute ethanol (EtOH) was purchased from Hengxing Chemical Reagent Co., Ltd. (Tianjin, China). Deionized water was prepared in the laboratory. All chemicals were used as received.

Amorphous Nextel™ 312 ceramic fibers with diameters ranged from 10 to 12 μm were offered by 3 M Company (Saint Paul, USA). The fibers are composed of 62 wt% Al_2O_3, 14 wt% B_2O_3 and 24 wt% SiO_2 as reported [7,8].

2.2. Sample preparation

Firstly, BAA, TEOS, H_2O and EtOH with mass percentages of 15, 7.2, 38.9 and 38.9 wt% were mixed together. Then the mixture was stirred at 40 °C for 12 h to obtain homogeneous monophasic mullite sol. The sol was filtered after standing for 72 h to remove large impurity particles. After that, the purified sol was concentrated using a rotary evaporator to adjust to suitable viscosity to acquire the spinnable sol. The green fibers were hand drawn using a glass rod and collected by a rotating roller. The resulting fibers were dried at 25 °C for 12 h and then were performed in a muffle furnace. They were heated to 800 °C under air circumstance and maintained for 1 h to acquire MBM fibers.

The as-received 312 fibers were firstly desized at 600 °C for 1 h in air. Then the as-prepared MBM fibers and desized 312 fibers were heat treated from 1000 °C to 1400 °C with a dwell time of 1.5 h. All the samples were cooled down to room temperature and collected for further characterization.

2.3. Characterization

Thermal analysis was performed on a STA449C thermoanalyzer (Netzsch, German) at a heating rate of 10 °C/min. X-ray powder diffraction (XRD) data of the mullite fibers were recorded by a diffractometer (SIEMENS, D500, German) in the region of $10 < 2\theta < 80°$. The chemical structures of the heat-treated samples were investigated by Fourier transform infrared (FT-IR) absorption spectra measured by a Model 6700 spectrometer (Nicolet, USA) using the KBr pellet method. The fiber morphology was observed by a Helios NanoLab G3 UC scanning electron microscopy (SEM) (FEI, Czech). The crystal grains of the crystallized fibers was observed by JEM-2100F transmission electron microscopy (TEM) (JEOL, Japan). Image J (NIH, USA) was used to calculate the fiber diameters and grain sizes.

The apparent densities (ρ) of the fiber products were measured on the basis of the ISO 18754:2013 standard using an XSE105DU laboratory balance (Mettler Toledo, Switzerland). After measuring the weights in the air, the fibers were weighted in alcohol, and then the density were calculated. The filament tensile strength was measured by an XS(08)XT-3 fiber strength tester (XuSai, China) using a traveling speed of 1 mm/min and performed at room temperatures. The gauge length of the fiber for the tensile test was 15 μm. Twenty samples were tested to acquire the strength values. The cross-sectional area of each tested fiber was measured using SEM measurement.

3. Results and discussion

3.1. Preparation and characterization of MBM fibers

The thermal behavior of the green fibers is assessed by TG and DSC and shown in Fig. 1. Two major mass losses occurred during the heating process as evidenced from the TG curve. The first mass loss of ~ 18.2 wt % at 160 °C was caused by the removal of crystal water, which corresponded to an endothermic peak located at 102 °C in the DSC curve. While from 160 °C to 664 °C, the second mass loss of ~ 30.3 wt% was

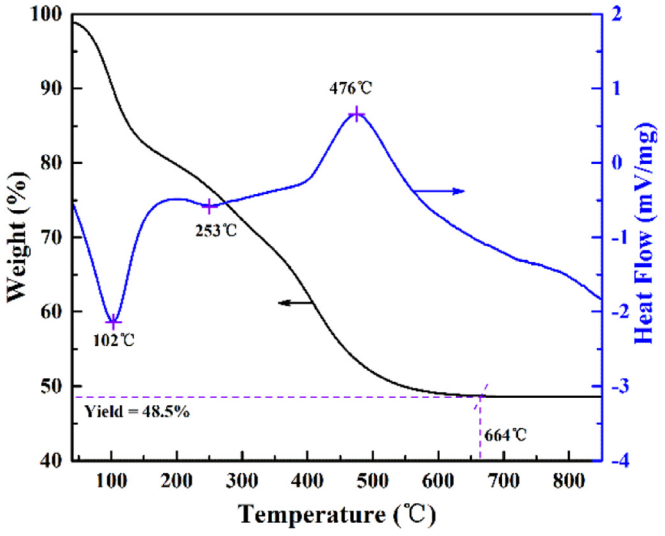

Fig. 1. TG-DSC curves of the green fibers at a heating rate of 10 °C min^{-1}.

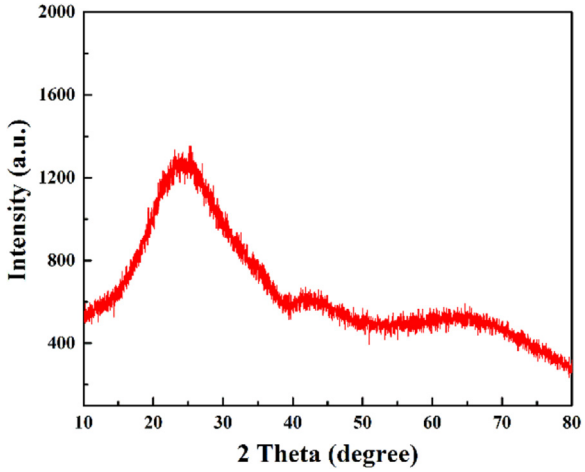

Fig. 2. XRD pattern of the as-prepared MBM fibers.

induced by the decomposition of boric acid and organics. This was associated with an endothermic peak at 253 °C and an exothermic peak at 476 °C in the DSC. No evident mass loss was observed at temperatures higher than 664 °C, revealing that the organics had been removed. Accordingly, no other exothermic peak was found below 850 °C in the DSC curve. It could be deduced that the MBM fibers were in the amorphous state since they were prepared at 800 °C. This was confirmed by the XRD pattern displayed in Fig. 2, that the peaks were broad.

Fig. 3 displays the SEM images of green fibers and MBM fibers. As revealed in Fig. 3(a), the green fibers were continuous and uniform, with an average diameter of 11.24 μm. Fig. 3(b) showed that the fiber surface was very smooth and no defects like voids or cracks generated during the fiber drawing and drying process. They had superior structural and morphological stability under room temperature even the humidity up to 65%. The as-prepared MBM fibers, as evident from Fig. 3(c) and (d), retained smooth and defect-free surface features. No obvious pores generated in the fiber inner after thermal treatment. The average fiber diameter decreased to 7.33 μm due to the decomposition of the organic compounds. The ideal surface characteristics and fine diameters were beneficial to acquire the fiber products with high mechanical properties.

Table 1
Density and filament tensile strength of as-prepared MBM fibers and desized 312 fibers.

Fiber sample	Manufacturing method	Density (g/cm^3)	Tensile strength (GPa)
MBM	Hand drawing	2.69 ± 0.07	1.18 ± 0.17
312	Dry spinning	2.72 ± 0.05	1.55 ± 0.14

The density and filament tensile strength of as-prepared MBM fibers and desized 312 fibers are listed in Table 1. The density of MBM fibers was almost the same with that of 312 fibers, implying their good lightweight feature. The tensile strength of as-prepared MBM fibers was 1.18 ± 0.17 GPa, which was lower than that of the 312 fibers. A possible explanation for this was the different manufacturing methods employed. For commercial mullite fibers, fiber processing is accomplished by dry spinning technique. During the preparing process, some adopted unique technologies including coating organic sizes on green fibers, exerting tension on amorphous inorganic fibers, etc. [16,19] might reduce the defects and improve the mechanical properties of the fibers. However, those technologies were not carried out for hand drawing ceramic fibers in present study. In other words, there was still room for strength improvement after optimizing the manufacturing method of our MBM fibers.

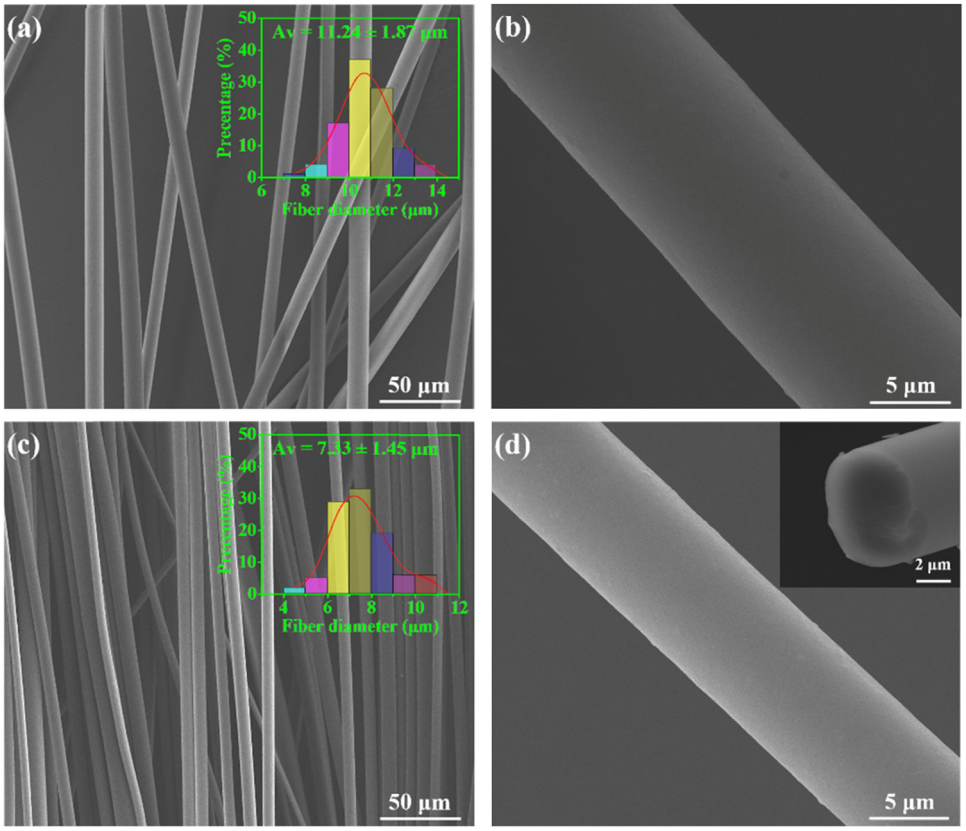

Fig. 3. SEM images of (a) (b) as-spun green fibers and (c) (d) as-prepared MBM fibers. The inserts in (a) and (c) show the diameter distribution histograms, and in (d) display the fiber fracture morphology.

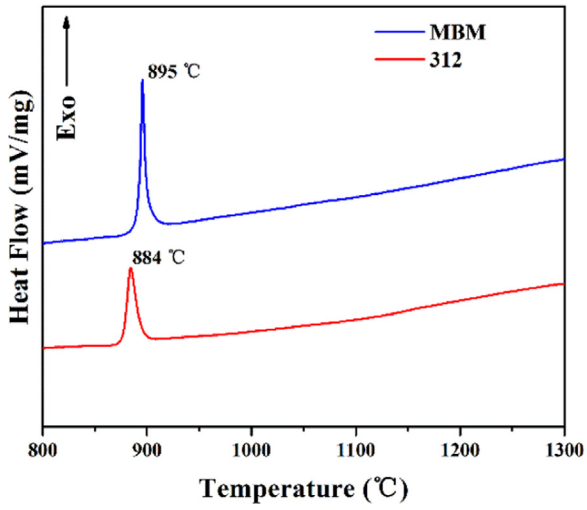

Fig. 4. DSC curves for amorphous MBM fibers and 312 fibers in the range of 800–1300 °C.

3.2. Microstructure evolution at elevated temperatures

The DSC curves for amorphous MBM and 312 fibers in the range of 800–1300 °C are shown in Fig. 4. The peak temperature assigned to $Al_4B_2O_9$ phase for amorphous MBM fibers was 895 °C, while that for 312 fibers was 884 °C. Such results implied that SiO_2 could affect the crystallization despite it did not participate in the crystal phase formation. The influence mechanism was that amorphous SiO_2 particles could hinder the reaction between Al_2O_3 and B_2O_3 during crystallization. For MBM fibers, according to the synthesized route of precursor sol, Al, Si and B elements distributed more uniformly, resulting in the more uniform dispersion of amorphous Al_2O_3, SiO_2, and B_2O_3 particles. Therefore, the hindrance effects of SiO_2 were stronger, which led to the higher formation temperature of $Al_4B_2O_9$ phase.

For each sample, no crystallization peak emerged in the DSC curves even the heating temperature reached 1300 °C, revealing that less crystallization heat released during the further phase transformation processes. In Al_2O_3-SiO_2-B_2O_3 ternary ceramics, mullite would form when calcination temperatures increased [20,21]. Therefore, the formation temperatures of mullite for the two samples could not be ascertained by the DSC method. As well known, the TO_4 (T = Al or Si) units normally act as the nucleation sites of mullite. Thus, the formation of the TO_4 units is an indicator that mullite has emerged [22]. To ascertain the formation temperature of the mullite phase, FT-IR spectra of the two fibers in the range of 1000–500 cm^{-1} after heat-treatment at temperatures of 1000–1100 °C are recorded and displayed in Fig. 5. In Fig. 5(a), a weak absorption band at 737 cm^{-1} was observed and assigned to the bending vibration of T-O-T in TO_4 units for the sample prepared at 1075 °C. The band became more obvious for the fibers heat treated at 1100 °C but not found after heat-treatment at 1050 °C. These results revealed that mullite formed in the temperature interval from 1050 to 1075 °C for MBM fibers. It was apparent that the formation temperatures were higher than that of pure monophasic mullite. This is because there was no enough Al_2O_3 reacted with SiO_2 before the decomposition of alumina borate phases. With respect to 312 fibers, the same conclusion could be drawn from Fig. 5(b) that mullite also formed at the same temperature interval. For diphasic mullite with 5 wt% borate, the formation temperature of mullite decreased from ~ 1350 °C to ~ 1200 °C [15]. In view of those facts, the detected mullite formation temperature for 312 fibers was reasonable. In conclusion, the different synthesis routes of mullite sol exerted little influence on mullite formation temperatures for Al_2O_3-SiO_2-B_2O_3 ternary ceramics with Al_2O_3:SiO_2:B_2O_3 mol ratio of 3:2:1.

Fig. 6 shows the XRD patterns of MBM fibers and 312 fibers after heat-treatment at elevated temperatures. It is shown that the two fibers consisted of $Al_4B_2O_9$ (card #47-0319) phase and amorphous SiO_2 at 1000 °C. After heat-treated at 1100 °C, four weak diffraction peaks were observed at the 2θ of 20.3, 23.7, 48.5 and 75.1°. The former two peaks were clearly seen in the inserts. This reveals that $Al_4B_2O_9$ had transformed to $Al_{18}B_4O_{33}$ (card #32-0003). FT-IR results had shown that mullite had formed at this temperature. With the heat-treatment temperatures increased, the diffraction peaks at ~ 26° split into two peaks

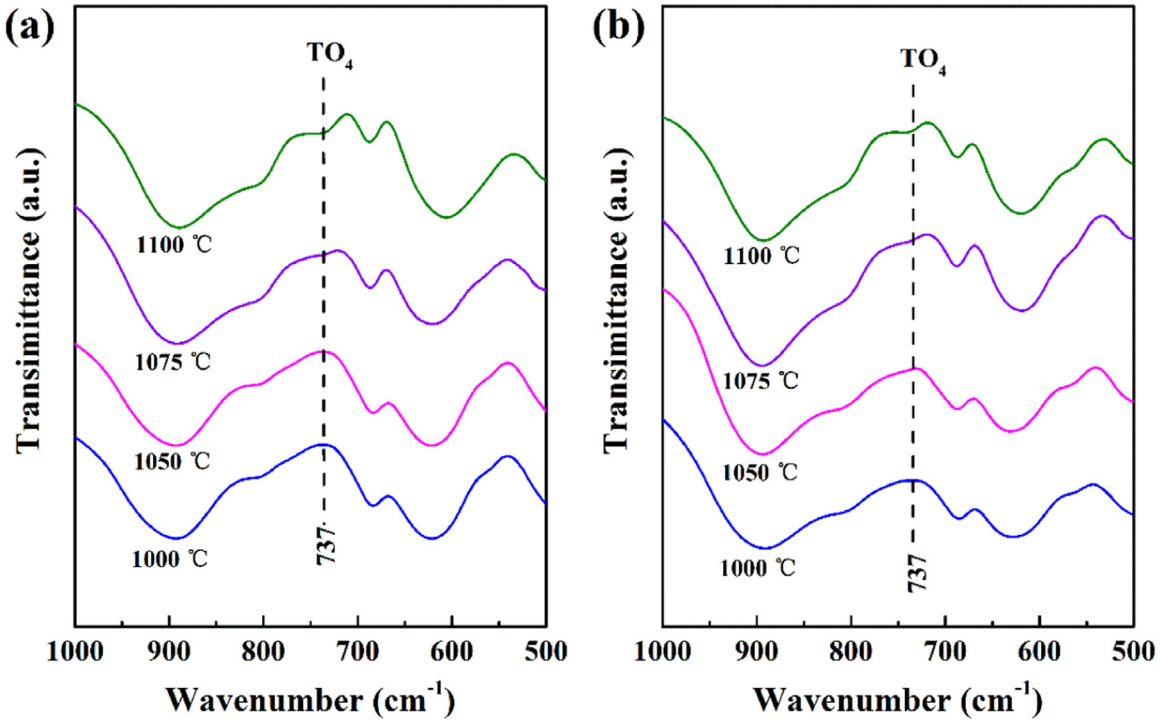

Fig. 5. FT-IR spectra of (a) MBM fibers and (b) 312 fibers in the range of 1000–500 cm^{-1} after heat-treatment at temperatures of 1000–1100 °C.

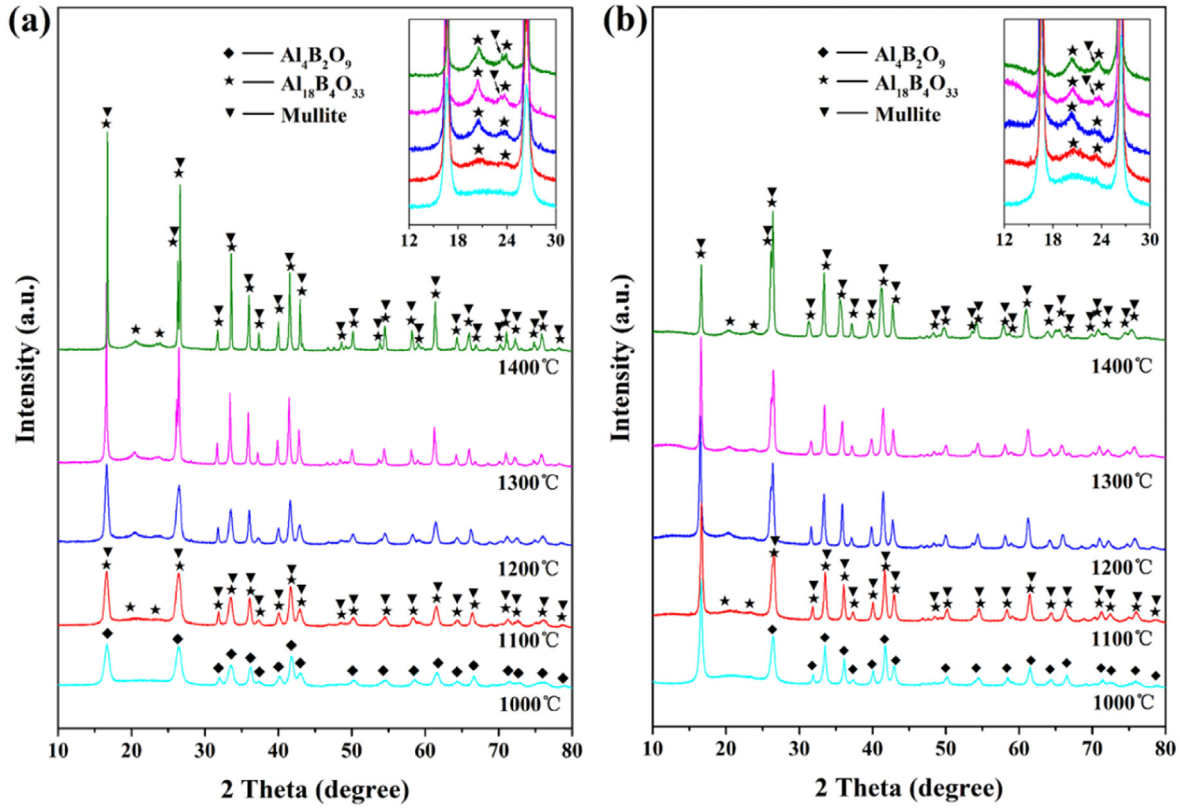

Fig. 6. XRD patterns for (a) MBM fibers and (b) 312 fibers after heat-treatment at elevated temperatures. The inserts show the patterns in the region of $12 < 2\theta < 30^{\circ}$.

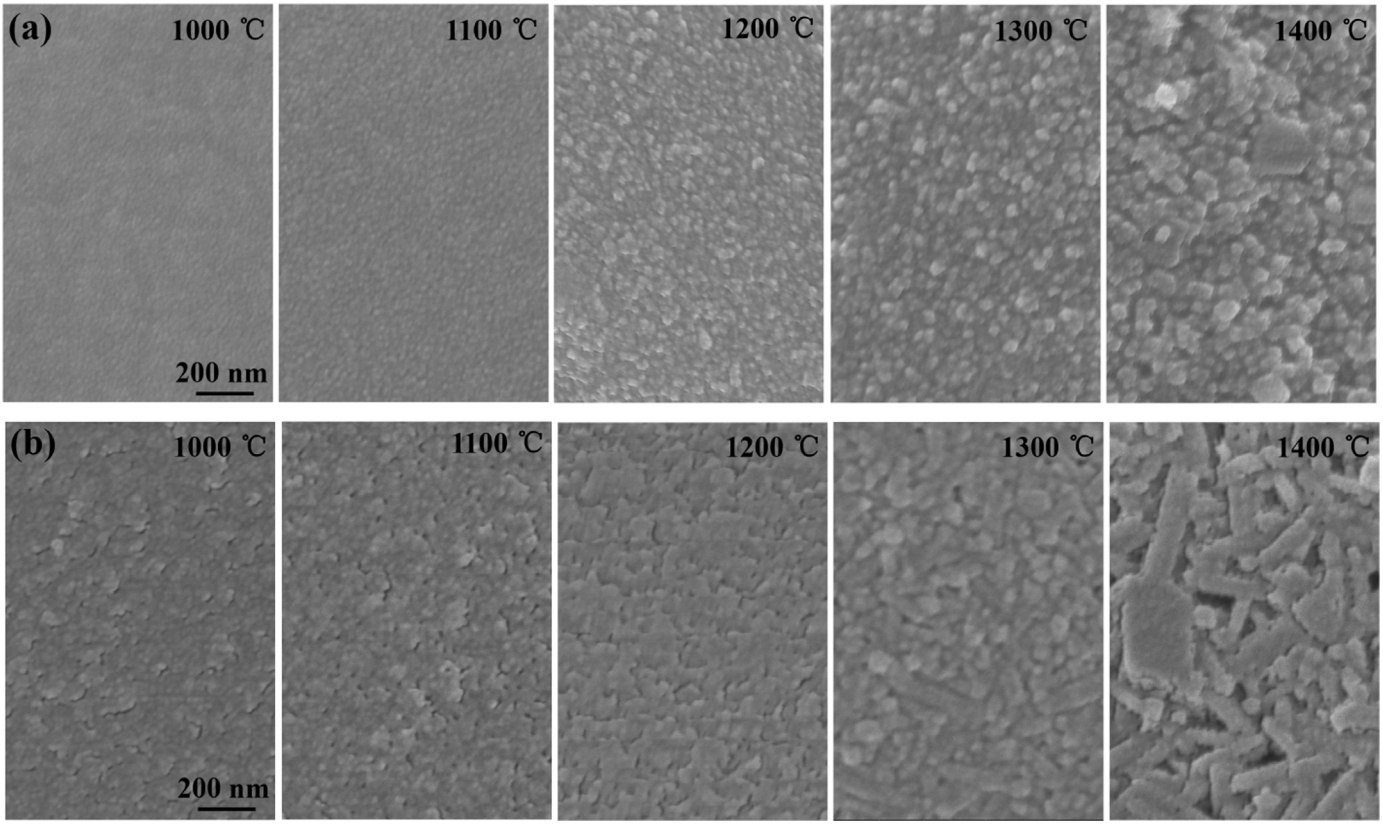

Fig. 7. SEM images of (a) MBM fibers and (b) 312 fibers after heat-treatment at elevated temperatures.

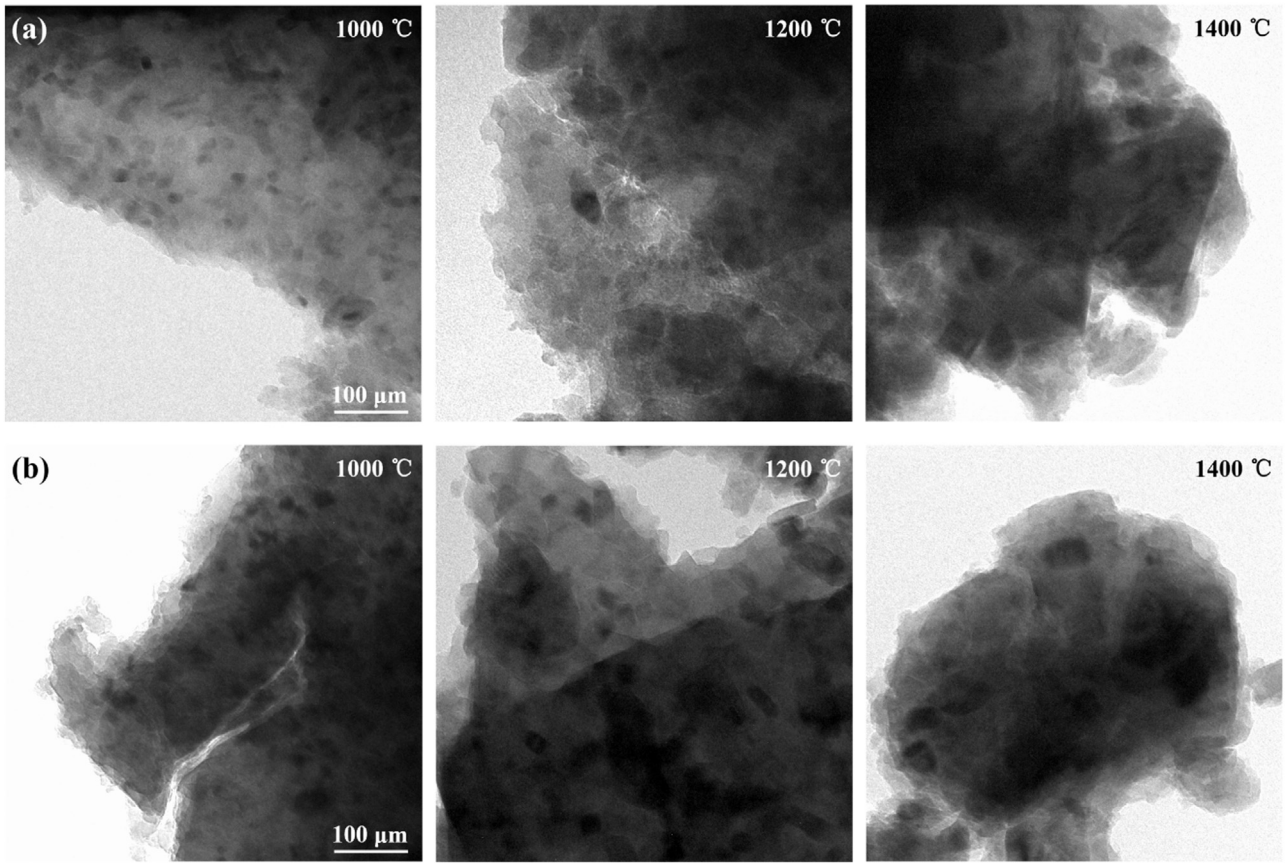

Fig. 8. TEM images of (a) MBM fibers and (b) 312 fibers after heat-treatment at elevated temperatures.

Table 2
Average grain size of MBM fibers and 312 fibers heat-treated at elevated temperatures derived from the TEM observations.

Fiber sample	Average grain size (nm)		
	1000 °C	1200 °C	1400 °C
MBM	14.11 ± 3.47	25.41 ± 3.99	56.67 ± 9.13
312	23.52 ± 4.86	39.28 ± 8.44	63.90 ± 10.38

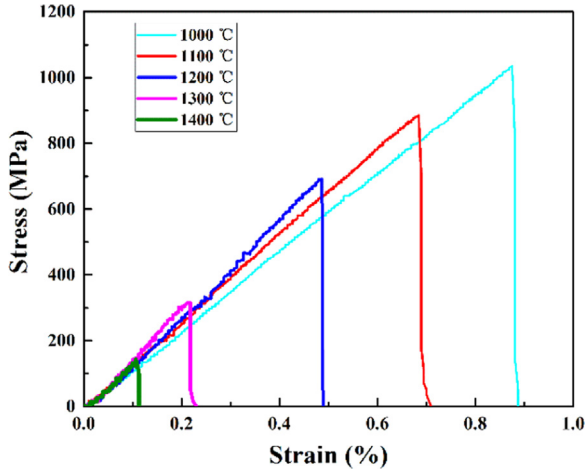

Fig. 9. Typical stress-strain curves for MBM fibers after heat-treatment at elevated temperatures.

and the peak intensities increased steadily, indicating that the crystallinity and amount of mullite increased. As known to us, most of the diffraction lines of $Al_{18}B_4O_{33}$ and mullite overlapped due to the same crystal structure and similar lattice parameters [17,18]. Therefore, to ascertain the accurate amount of the two phases by Rietveld refinement of the XRD data was impossible. However, the dominant phase could be confirmed by the intensities of the diffraction peaks. For the two samples, $Al_{18}B_4O_{33}$ was the dominant phase when the temperatures increased to 1300 °C since the relative intensities of the first two strong diffraction peaks located at the 2θ of 16° and 26° did not reverse [12]. After heat-treatment at 1400 °C, the XRD results for MBM and 312 fibers were different. As shown in Fig. 6(a), $Al_{18}B_4O_{33}$ was still the dominant phase. While the pattern displayed in Fig. 6(b) revealed that mullite had become the dominant phase. As we know, $Al_{18}B_4O_{33}$ would decompose generally with the increasing temperature. Therefore, it could be concluded that the decomposition rate in MBM fibers was lower. As had been discussed in our previous works, amorphous SiO_2 would always exist in fibers with Al_2O_3:SiO_2:B_2O_3 mol ratio of 3:2:1 theoretically as long as alumina borate phase did not decomposed completely [18]. So the content of amorphous SiO_2 in MBM fibers heat treated at elevated temperatures was higher. Definitely, the higher amorphous SiO_2 contents favored to stabilize the fiber structure.

SEM images of MBM fibers and 312 fibers after heat-treatment at elevated temperatures are shown in Fig. 7. For MBM fibers, as could be seen from Fig. 7(a), the surface was smooth after heat-treatment at 1000 °C even at the crystallization of $Al_4B_2O_9$ phase. With increased temperatures, the surface became rougher and rougher due to the grain growth. It was evident that the grains possessed similar polygonal shapes in spite of the sizes. With respect to 312 fibers, it could be found in Fig. 7(b) that the surface with many tiny cracks was rough after heat-treatment at 1000 °C. Such defects would not vanish even at the heat-treated temperature reached 1200 °C. At 1300 °C, those tiny cracks

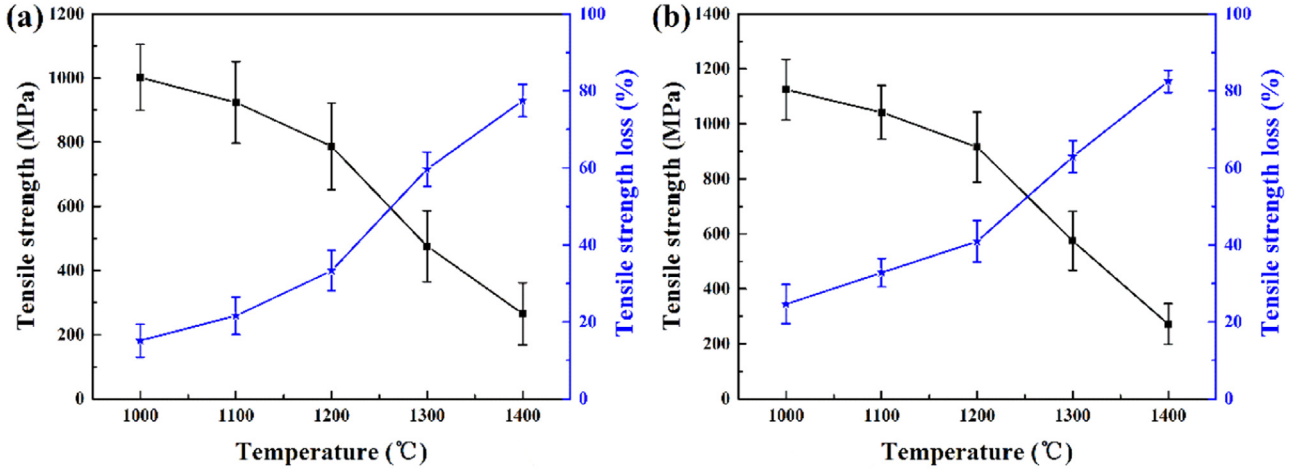

Fig. 10. Tensile strength and tensile strength loss of (a) MBM fibers and (b) 312 fibers after heat-treatment at elevated temperatures.

disappeared but many irregular grains generated. In comparison, the grain sizes in 312 fibers were much larger than that in MBM fibers. When the heat-treatment temperature was 1400 °C, most grains grew to be elongated and oblong shapes, and apparently, their sizes were the largest among all the samples. The SEM results were further confirmed by the TEM observation. Fig. 8 shows the TEM images of MBM fibers and 312 fibers heat-treated at 1000, 1200 and 1400 °C, and Table 2 lists the corresponding average grain sizes. As the temperature went up from 1000 °C to 1400 °C, the average grain size for MBM fibers increased from 14.11 nm to 56.67 nm, and that for 312 fibers increased from 23.52 nm to 63.90 nm. When the heat-treatment temperatures were same, the crystal grains in MBM fibers were smaller than those in 312 fibers. Based on these analyses, we concluded that MBM fibers had better structural stability than 312 fibers under high-temperature conditions.

3.3. Filament tensile strength for heat-treated fibers

Typical stress-strain curves for MBM fibers after heat-treatment at elevated temperatures are displayed in Fig. 9. Since 312 fibers showed similar tensile behaviors, their stress-strain curves were not shown here. It was clear that all the fibers exhibited linear elasticity until brittle fracture occurred. Such results were also the same with filament tensile behaviors of oxide ceramic fibers in other researches [6,23]. The filament tensile strength and strength loss of the heat treated MBM and 312 fibers are shown in Fig. 10. A decreasing tendency on tensile strength and an increasing tendency on strength loss for both fibers were observed with the increase of heat-treatment temperatures. Under the same heat-treatment temperatures, the strength values of MBM fibers were higher, the strength loss percentage was also higher. After heat treated at 1000 °C, the strength loss percentage was 24.6% for 312 fibers heat treated while it was 15.1% for MBM fibers. After the heat-treatment at 1400 °C, the two fibers lose 82.5% and 77.5% of the original strength values, respectively. Therefore, the MBM fibers owned more stable mechanical properties under high temperature circumstance in spite of the lower tensile strength.

4. Conclusion

Boron-containing mullite fibers with the same chemical composition with Nextel™ 312 fibers were successfully prepared through the simple, stable and low-cost monophasic mullite sol-gel route. Spinning dope was acquired by concentrating the monophasic sol to a suitable viscosity. The hand drawing green fibers with an average diameter of ~ 11 μm were continuous, uniform and smooth. Amorphous MBM fibers with a density of 2.71 ± 0.07 g/cm^3 and a tensile strength of 1.18 ± 0.17 GPa were obtained by pyrolysis of the green fibers at an ending temperature of 800 °C. $Al_4B_2O_9$ formed first at 895 °C, which was higher than that of 312 fibers. Mullite formed between the temperature range from 1050 to 1075 °C. Alumina borate phases were the dominant phase all through as heat-treatment temperatures increased. As compared with Nextel™ 312 fibers, the grain sizes were smaller, the morphological characteristics were better and the tensile strength losses were lower. These evidences indicated that our MBM fibers had better thermal stability than Nextel™ 312 fibers, and could be implemented in high-temperature conditions.

Acknowledgements

The authors gratefully acknowledge the financial support from the “Chang Jiang Scholars Program” of the Ministry of Education of China (Grant no. T2011119).

References

[1] A.R. Bunsell, M.H. Berger, Fine diameter ceramic fibres, J. Eur. Ceram. Soc. 20 (2000) 2249–2260.
[2] F. Deléglise, M.H. Berger, D. Jeulin, A.R. Bunsell, Microstructural stability and room temperature mechanical properties of the Nextel 720 fibre, J. Eur. Ceram. Soc. 21 (2001) 569–580.
[3] D. Schawaller, B. Clauß, M.R. Buchmeiser, Ceramic filament fibers - a review, Macromol. Mater. Eng. 297 (2012) 502–522.
[4] R.S.M. Almeida, E.L. Bergmüller, B.G.F. Eggert, K. Tushtev, T. Schumacher, H. Lührs, B. Clauß, G. Grathwohl, K. Rezwan, Thermal exposure effects on the strength and microstructure of a novel mullite fiber, J. Am. Ceram. Soc. 99 (2016) 1709–1716.
[5] H. Schneider, Basic properties of mullite, in: H. Schneider, S. Komarneni (Eds.), Mullite, Wiley-VCH, Weinheim, 2005, pp. 141–215.
[6] X. Dong, Z. Chen, A. Guo, J. Liu, X. Wang, C. Chen, Mechanical and interfacial behavior of single mullite fiber and mullite fiber-based porous ceramics, Ceram. Int. 44 (2018) 14446–14456.
[7] D.D. Johnson, Nextel 312 ceramic fiber from 3M, J. Ind. Text. 10 (1982) 282–296.
[8] T.L. Tompkins, Ceramic oxide fibers: building blocks for new applications, Ceram. Ind. 144 (1995) 45–48.
[9] N. Chawla, M. Kerr, K.K. Chawla, Monotonic and cyclic fatigue behavior of high-performance ceramic fibers, J. Am. Ceram. Soc. 88 (2005) 101–108.
[10] Y. Wang, H. Cheng, H. Liu, J. Wang, Microstructure and room temperature mechanical properties of mullite fibers after heat-treatment at elevated temperatures, Mater. Sci. Eng. A 578 (2013) 287–293.
[11] X. Dong, G. Sui, A. Guo, H. Du, J. Liu, Synthesis and properties of lightweight flexible insulant composites with a mullite fiber-based hierarchical heterostructure, Chem. Eng. J. 277 (2015) 159–167.
[12] H.G. Sowman, Alumina–boria–silica ceramic fibers from the sol-gel process, in: L.C. Klein (Ed.), Sol–Gel Technoloy For Thin Films, Fibers, Performs, Electronics, And Specialty Shapes, Noyes, Park Ridge, NJ, 1988, pp. 162–182.
[13] L.S. Cividanes, T.M.B. Campos, L.A. Rodrigues, D.D. Brunelli, G.P. Thim, Review of mullite synthesis routes by sol-gel method, J. Sol-Gel Sci. Technol. 55 (2010) 111–125.
[14] S.H. Hong, G.L. Messing, Mullite transformation kinetics in P_2O_5-, TiO_2-, and B_2O_3-doped aluminosilicate gels, J. Am. Ceram. Soc. 80 (1997) 1151–1159.

[15] S.H. Hong, W. Cermignani, G.L. Messing, Anisotropic grain growth in seeded and B_2O_3-doped Diphasic mullite gels, J. Eur. Ceram. Soc. 16 (1996) 133–141.
[16] H.G. Sowman, Aluminum borate and aluminum borosilicate articles, U.S. Patent 3, 795,524, 1974.
[17] G. Zhang, Z. Fu, Y. Wang, H. Wang, W. Wang, J. Zhang, S.W. Lee, K. Niihara, Boron-doped mullite derived from single-phase gels, J. Eur. Ceram. Soc. 30 (2010) 2435–2441.
[18] X. Song, W. Liu, S. Xu, J. Wang, B. Liu, Q. Cai, S. Tang, Y. Ma, Microstructure and elastic modulus of electrospun Al_2O_3-SiO_2-B_2O_3 composite nanofibers with mullite-type structure prepared at elevated temperatures, J. Eur. Ceram. Soc. 38 (2018) 201–210.
[19] A. Borer, G.P. Krogseng, Method of firing dry spun refractory oxide fibers, U.S. Patent 3,760,049, 1973.
[20] H. Lührs, R.X. Fischer, H. Schneider, Boron mullite: formation and basic characterization, Mater. Res. Bull. 47 (2012) 4031–4042.
[21] K.J. Griesser, A. Beran, D. Voll, H. Schneider, Boron incorporation into mullite, Mineral. Petrol. 92 (2008) 309–320.
[22] J. Leivo, M. Lindén, J.M. Rosenholm, M. Ritola, C.V. Teixeira, E. Levänen, T.A. Mäntylä, Evolution of aluminosilicate structure and mullite crystallization from homogeneous nanoparticulate sol-gel precursor with organic additives, J. Eur. Ceram. Soc. 28 (2008) 1749–1762.
[23] H.G. Sowman, D.D. Johnson, Ceramic oxide fibers, Ceram. Eng. Sci. Proc. 6 (1985) 1221–1230.